metals

MDPI

Article

Leaching Manganese Nodules in an Acid Medium and Room Temperature Comparing the Use of Different Fe Reducing Agents

David Torres [1,2], Luís Ayala [3], Manuel Saldaña [1], Manuel Cánovas [1], Ricardo I. Jeldres [4], Steven Nieto [4], Jonathan Castillo [5], Pedro Robles [6] and Norman Toro [1,3,*]

1 Departamento de Ingeniería Metalúrgica y Minas, Universidad Católica del Norte, Av. Angamos 610, Antofagasta 1270709, Chile; david.Torres@sqm.com (D.T.); manuel.saldana@ucn.cl (M.S); manuel.canovas@ucn.cl (M.C.)

2 Department of Mining, Geological and Cartographic Department, Universidad Politécnica de Cartagena, 30203 Cartagena, Spain

3 Faculty of Engineering and Architecture, Universidad Arturo Pratt, Almirante Juan José Latorre 2901, Antofagasta 1244260, Chile; luisayala01@unap.cl

4 Departamento de Ingeniería Química y Procesos de Minerales, Universidad de Antofagasta, Antofagasta 1240000, Chile; ricardo.jeldres@uantof.cl (R.I.J.); stevennietomejia@gmail.com (S.N.)

5 Departamento de Ingeniería en Metalurgia, Universidad de Atacama, Av. Copayapu 485, Copiapó 1531772, Chile; jonathan.castillo@uda.cl

6 Escuela de Ingeniería Química, Pontificia Universidad Católica de Valparaíso, Valparaíso 2340000, Chile; pedro.robles@pucv.cl

* Correspondence: ntoro@ucn.cl; Tel.: +56-552651021

Received: 23 October 2019; Accepted: 4 December 2019; Published: 6 December 2019

Abstract: The deposits of Fe-Mn, in the seabed of the planet, are a good alternative source for the extraction of elements of interest. Among these are marine nodules, which have approximately 24% manganese and may be a solution to the shortage of high-grade ores on the surface. In this investigation, an ANOVA analysis was performed to evaluate the time independent variables and MnO_2/reducing agent in the leaching of manganese nodules with the use of different Fe reducing agents (FeS_2, Fe^{2+}, Fe^0 and Fe_2O_3). Tests were also carried out for the different reducing agents evaluating the MnO_2/Fe ratio, in which the Fe^0 (FeC) proved to be the best reducing agent for the dissolution of Mn from marine nodules, achieving solutions of 97% in 20 min. In addition, it was discovered that at low MnO_2/Fe ratios the acid concentration in the system is not very relevant and the potential and pH were in ranges of −0.4–1.4 V and −2–0.1 favoring the dissolution of Mn from MnO_2.

Keywords: MnO_2; acid media; ANOVA; dissolution

1. Introduction

Deposits of ferromanganese (Fe-Mn) are found in the oceans around the world [1–4]. These deposits contain ferromanganese crusts, as well as cobalt-rich crusts and manganese nodules [5–7]. These marine resources are found mainly in the Pacific, Atlantic and Indian Ocean [8], and are formed by precipitation processes of Mn and Fe oxides around a nucleus, which is commonly composed of a fragment of an older nodule [9]. Manganese nodules also called polymetallic nodules because they are associated with large reserves of metals, such as Cu, Ni, Co, Fe and Mn, the latter being the most abundant, with an average content of around 24% [10]. In addition to the aforementioned elements, considerable quantities of Te, Ti, Pt and rare earths can also be found [11]. These nodules might be good source of manganese in the industry for high demand in steel production [12–14].

To extract Mn and other metals of interest from marine nodules, the use of a reducing agent is necessary [15,16]. Studies have used different reducing agents, such as, wastewater from the manufacture of alcohol from molasses [17], coal [18], H_2SO_3 [19,20], pyrite [21], sponge iron [22] and cast iron slag magnetite [23]. Iron has shown to be a good reducing agent for manganese extraction, from those, due to its low cost and abundance [23]. Several studies have been carried out to evaluate the effect of iron as a reducing agent in leaching in acid media of marine nodules [21,24]. For studies in acidic media and iron, it has been reported that the best results for extracting manganese are obtained by increasing the amounts of Fe in the Mn/Fe ratio and working at low acid concentrations [22,23].

In the studies by Kanungo [21,25], an acid leaching (HCl) was conducted at different temperatures with the addition of pyrite as a reducing agent achieving 50% manganese extractions. The author concluded that, in a moderately acidic medium, pH of 1.5, the Fe (II) and Fe (III) ratio in the system remains essentially constant up to 50 min above, which the ratio tends to increase exponentially. From this, it is suggested that the reduction of MnO_2 by ferrous ions occurs at a faster rate than the oxidation of pyrite generating ferric ions. For the dissolution of Mn with the use of pyrite in acidic media, the following series of reactions is proposed [21]:

$$3FeS_2 + 4H_2SO_4 = 3FeSO_4 + 4H_2O + 7S \quad (1)$$

$$6FeSO_4 + 4H_2SO_4 = 3Fe_2(SO_4)_3 + 4H_2O + S \quad (2)$$

$$2FeS_2 + 4H_2SO_4 = Fe_2(SO_4)_3 + 4H_2O + 5S \quad (3)$$

$$15MnO_2 + 2FeS_2 + 14H_2SO_4 = Fe_2(SO_4)_3 + 15MnSO_4 + 14H_2O \quad (4)$$

For the use of ferrous ions, Zakeri et al. [24] indicated that when working in a molar ratio of Fe^{2+}/MnO_2 of 3/1, a molar ratio of H_2SO_4/MnO_2 of 2/1 and a mineral particle size of −60 + 100 Tyler mesh, 90% extractions of Mn can be obtained in less than 20 min at a temperature of 20 °C. In their work they proposed the following series of reactions:

$$MnO_2 + 4H^+ + 2e^- = Mn^{2+} + 2H_2O \quad (5)$$

$$2Fe^{2+} = 2Fe^{3+} + 2e^- \quad (6)$$

$$MnO_2 + 2Fe^{2+} + 4H^+ = Mn^{2+} + 2Fe^{3+} + 2H_2O \quad (7)$$

Subsequently, Bafghi et al. [22] conducted a similar experiment but with the use of Fe sponge, where he compared the results reported by Zakeri et al. [24] and indicated that under the same operating conditions, sponge Fe delivers better results than the addition of ferrous ions, because the metal of Fe allows us to have a high activity ratio through the regeneration of ferrous ions. For the dissolution of Mn with the use of Fe (s), the following reactions are presented [22]:

$$Fe\ (s) + 2H^+ = Fe + H_2\ (g) \quad (8)$$

$$Fe\ (s) + 2Fe^{3+} = 3Fe^{2+} \quad (9)$$

$$MnO_2\ (s) + 2Fe^{2+} + 4H^+ = Mn^{2+} + 2Fe^{3+} + 2H_2O \quad (10)$$

$$MnO_2\ (s) + 2Fe\ (s) + 8H^+ = Mn^{2+} + 2Fe^{3+} + 2H_2O + 2\ H_2\ (g) \quad (11)$$

$$MnO_2\ (s) + Fe\ (s) + 4H^+ = Mn^{2+} + Fe^{2+} + 2H_2O \quad (12)$$

$$MnO_2\ (s) + 2/3Fe\ (s) + 4H^+ = Mn^{2+} + 2/3Fe^{3+} + 2H_2O \quad (13)$$

In the studies carried out by Toro et al. [23,26] smelting slag was used, taking advantage of the Fe_2O_3 presented in these to reduce MnO_2 in an acid medium. It was concluded that the ratios of MnO_2/Fe = 1/2 and 1 M H_2SO_4 significantly shorten the dissolution time of manganese (from 30 to

5 min). In addition, the authors indicated that the particle size is not as significant in Mn solutions as in the concentration of H_2SO_4. For the dissolution of Mn with the use of Fe_2O_3 in acid media, the following series of reactions is presented:

$$Fe_2O_3\ (s) + 3H_2SO_4 = Fe_2(SO_4)_3\ (s) + 3H_2O \quad (14)$$

$$Fe_3O_4\ (s) + 4H_2SO_4 = FeSO_4 + Fe_2(SO_4)_3\ (s) + 4H_2O \quad (15)$$

$$Fe_2(SO_4)_3\ (s) + 6H_2O = 2Fe(OH)_3\ (s) + 3H_2SO_4 \quad (16)$$

$$2FeSO_4 + 2H_2O = 2Fe\ (s) + 2H_2SO_4 + O_2\ (g) \quad (17)$$

$$2FeSO_4 + 2H_2SO_4 + MnO_2\ (s) = Fe_2(SO_4)_3\ (s) + 2H_2O + MnSO_4 \quad (18)$$

It is imperative to create innovative methods for the treatment of minerals that involve industrial waste reusing. Big mining companies are promoting recycling to generate a more sustainable sector. An example is the iron industry in China, where it is sought to reduce pollution by adding scrap in steelmaking [27]. Another example is mining in Chile, where companies like Collahuasi have recycling programs, in which they annually recover 3000 tons of scrap metal, 4 thousand kilos of electronic waste, 182 thousand units of plastic bottles and 680 kg of paper and cardboard [28]. Regarding steel scrap, the copper mining industry generates large amounts of this waste in the milling processes, but the steel balls or bars are discarded [29].

In this research, the leaching of MnO_2 to recover manganese with the use of different types of Fe reducing agents (pyrite, ferric ions, steel and magnetite) working under the same operating conditions was studied. The objective of this work is to find the most suitable iron reducing agent to extract manganese when working in an acidic environment and room temperature, with the novelty of testing the use of steel. A statistical analysis was conducted performed to evaluate the performance of the different selected reducers. Finally, the obtained results were compared in leaching tests over time, indicating which allow obtaining the best results.

2. Methodology

2.1. Manganese Nodule

The marine nodules used in this research were collected in the 1970s from the Blake Plateau in the Atlantic Ocean. The sample was reduced in size using a porcelain mortar and classified by mesh sieves until reaching a range between −140 + 100 µm. Later, it was analyzed chemically by atomic emission spectrometry via induction-coupled plasma (ICP-AES), developed in the Applied Geochemistry Laboratory of the Department of Geological Sciences of the Catholic University of the North, and its chemical composition was 0.12% of Cu, 0.29% Co and 15.96% Mn. Its mineralogical composition is presented in Table 1. Micro X-ray fluorescence spectrometry (Micro-XRF) is a method for elementary analysis of non-homogeneous or irregularly shaped samples, as well as small samples or even inclusions. The sample material was analyzed in a Bruker® M4-Tornado µ-FRX table (Fremont, CA, USA). This spectrometer consists of an X-ray tube (Rh-anode), and the system features a polycapillary X-ray optic, which concentrates the radiation of the tube in minimal areas, allowing a point size of 20 µm for Mo-K. The elementary maps created with the built-in software of the M4 Tornado ™ (Fremont, CA, USA), ESPRIT, indicate that the nodules were composed of fragments of pre-existing nodules that formed its nucleus, with concentric layers that precipitated around the core in later stages.

Table 1. Mineralogical analysis of the manganese nodule.

Component	MgO	Al_2O_3	SiO_2	P_2O_5	SO_3	K_2O	CaO	TiO_2	MnO_2	Fe_2O_3
Mass (%)	3.54	3.69	2.97	7.20	1.17	0.33	22.48	1.07	25.24	26.02

2.2. FeS_2

For this study, a cubic pyrite crystal obtained from the Navajún Mine (La Rioja, Spain) was used. This sample was reduced in size with the use of a cone crusher at laboratory level and later a sprayer. It was then classified through meshes sieves until reaching a size range of −75 + 53 µm. It was then analyzed chemically by atomic emission spectrometry via induction-coupled plasma (ICP-AES), developed in the Applied Geochemistry Laboratory of the Department of Geological Sciences of the Catholic University of the North. Table 2 shows the chemical composition of the samples.

Table 2. Chemical composition.

Component	Fe	S_2
Mass (%)	46.63	53.37

X-ray diffraction analyses (XRD) of the pyrite were performed on a Bruker D8 ADVANCE diffractometer (Billerica, MA, US) with Cu λ = 1.5406 Å radiation generated at 40 kV and 30 mA. The analysis and identification of the crystalline phases were obtained using the DIFFRAC.EVA V4.2.1 program, with the Powder Diffraction File of ICDD database (PDF-2 (2004)) (Billerica, MA, US). According to the initial qualitative analysis of XRD, the primary mineral phase in the samples was pyrite, whose main peaks are at 33.153°, 37.121° and 40.797°. These peaks correspond to those given in the reference pattern PDF 01-1295 (ICDD, 2004). As seen in Figure 1, the analysis showed the sample has a purity of 99.40%.

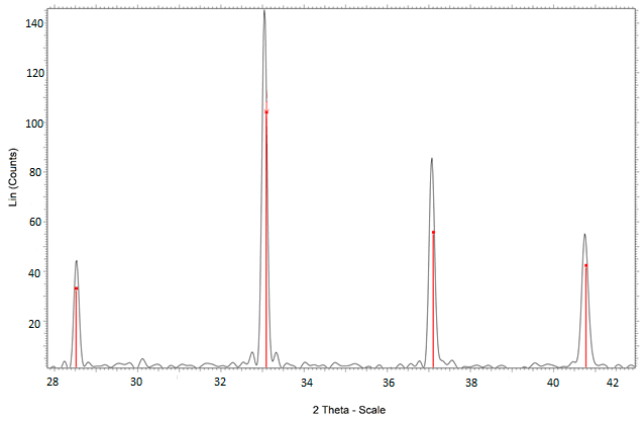

Figure 1. X-ray diffractogram for the pyrite mineral.

2.3. Fe_2O_3

The Fe_2O_3 used is found in tailings from the Altonorte Smelting Plant. Its size is in a range of −75 + 53 µm. The methods used to determine its chemical and mineralogical composition are the same as those used in marine nodules. Figure 2 and Table 3 shows the chemical species that use QEMSCAN (QEMSCAN has a database, which has the elemental composition, and density of the minerals that are detected. With this information, it is possible to obtain the elementary contribution of the measured sample), and several iron-containing phases are presented, while the Fe content is estimated at 41.9%.

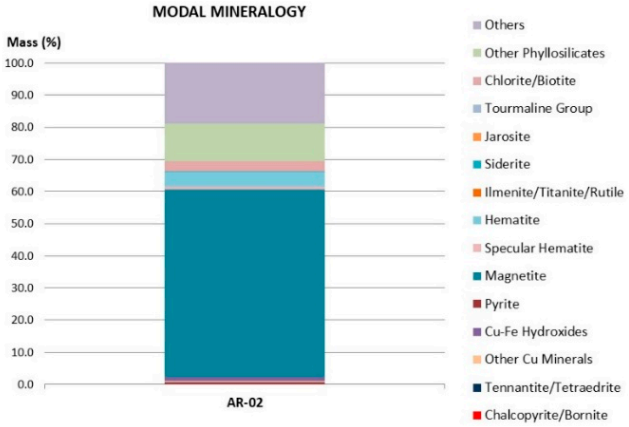

Figure 2. Detailed modal mineralogy.

Table 3. Shows the mineralogical composition of the tailings. The Fe in it was mainly in the form of magnetite.

Mineral	Amount % (w/w)
Chalcopyrite/Bornite $CuFeS_2/Cu_5FeS_4$	0.47
Tennantite/Tetrahedrite ($Cu_{12}As_4S_{13}/Cu_{12}Sb_4S_{13}$)	0.03
Other Cu Minerals	0.63
Cu–Fe Hydroxides	0.94
Pyrite (FeS_2)	0.12
Magnetite (Fe_3O_4)	58.52
Specular Hematite (Fe_2O_3)	0.89
Hematite (Fe_2O_3)	4.47
Ilmenite/Titanite/Rutile ($FeTiO_3/CaTiSiO_3/TiO_2$)	0.04
Siderite ($FeCO_3$)	0.22
Chlorite/Biotite ($Mg_3Si_4O_{10}(OH)_2(Mg)_3(OH)_6/K(Mg)_3AlSi_3O_{10}(OH)_2$)	3.13
Other Phyllosilicates	11.61
Fayalite (Fe_2SiO_4)	4.59
Dicalcium Silicate (Ca_2SiO_4)	8.3
Kirschsteinite ($CaFeSiO_4$)	3.4
Forsterita (Mg_2SiO_4)	2.3
Baritine ($BaSO_4$)	0.08
Zinc Oxide (ZnO)	0.02
Lead Oxide (PbO)	0.01
Sulfate (SO_4)	0.2
Others	0.03
Total	100

2.4. Steel (FeC)

A low carbon steel sheet (FeC; 0.25% C) from the steel supplier company Salomon Sack was used. This sample was reduced in size with the use of a cone crusher at laboratory level and later a pulverizer until reaching a size range between −75 + 53 µm.

2.5. Ferrous Ions

The ferrous ions used for this investigation ($FeSO_4 \times 7H_2O$) were the WINKLER brand (Santiago, Chile), with a molecular weight of 278.01 g/mol.

2.6. Reactor and Leaching Tests

The sulfuric acid used for the leaching tests was grade P.A., with 95–97% purity, a density of 1.84 kg/L and a molecular weight of 98.8 g/mol. The leaching tests were carried out in a 50 mL glass reactor with a 0.01 solid/liquid ratio in leaching solution. A total of 200 mg of Mn nodules were maintained

in agitation and suspension with the use of a 5 position magnetic stirrer (IKA ROS, CEP 13087-534, Campinas, Brazil) at a speed of 600 rpm. The tests were conducted at a room temperature of 25 °C, with variations in additives, particle size and leaching time. The tests performed in duplicate, measurements (or analyses) carried on 5 mL undiluted samples using atomic absorption spectrometry with a coefficient of variation ≤5% and a relative error between 5% and 10%. Measurements of pH and oxidation-reduction potential (ORP) of leach solutions were made using a pH-ORP meter (HANNA HI-4222, St. Louis, MO, USA). The solution ORP was measured in a combination ORP electrode cell composed of a platinum working electrode and a saturated Ag/AgCl reference electrode.

2.7. Estimation of Linear and Interaction Coefficients for Factorial Designs of Experiments of 2^3

Two independent variables were chosen for the factorial design of 36 experiments, where: time and ratio MnO_2/reducing agent represent the independent variables that explain the extraction of Mn for a certain type of reducing agent. The analysis through a factorial design allowed us to study the effect of the factors and their levels in a response variable, helping to understand which factors are the most relevant [30,31]. Four factorial designs were carried out that involved two factors with three levels each, with a total of 36 experimental tests (Table 4). The Minitab 18 software (version 18, Pennsylvania State University, State College, PA, USA) was used for modeling, experimental design and adjustment of a multiple regression [32].

Table 4. Experimental conditions.

Parameters/Values	Low	Medium	High
Time (min)	10	20	30
MnO_2/Reducing agent	2/1	1/1	1/2
Codifications	−1	0	1

The expression of the response variable according to the linear effect of the variables of interest and considering the effects of interaction and curvature, is shown in Equation (19).

$$Cu\ Recovery(\%) = \alpha + \sum_{i=1}^{n} \beta_i \times x_i + \sum_{i=1}^{n} \beta_i^2 \times x_i^2 + \beta_{1,2} \times x_1 \times x_2, \quad (19)$$

where α is the overall constant, x_i is the value of the level "i" of the factor, β_i is the coefficient of the linear factor x_i, β_i^2 is the coefficient of the quadratic factors, $\beta_{1,2}$ is the coefficient of the interaction, n are the levels of the factors and Mn recovery is the dependent variable.

Table 4 shows the values of the levels for each factor, while Table 5 shows the recovery obtained for each configuration.

Table 5. Experimental configuration and Mn extraction data.

Exp. No.	Time (min)	MnO_2/Reducing Agent Ratio	Mn Recovery (%; Reducing Agent)			
			FeS_2	Fe^{2+}	FeC	Fe_2O_3
1	10	2/1	4.12	20.52	22.31	33.33
2	10	1/1	8.51	40.69	44.00	50.23
3	10	1/2	10.66	80.27	87.13	71.00
4	20	2/1	8.34	27.80	30.22	39.22
5	20	1/1	12.69	63.11	67.43	57.32
6	20	1/2	19.21	90.18	97.00	73.21
7	30	2/1	15.84	40.32	41.99	42.55
8	30	1/1	19.11	70.00	74.33	72.96
9	30	1/2	26.32	93.50	97.34	75.14

3. Results

3.1. Statistical Analysis

From the analysis of the main components, the time and ratio factors MnO_2/Reducing agent showed a main effect, since the variation between the different levels affected the response in a different way, as shown in Figure 3.

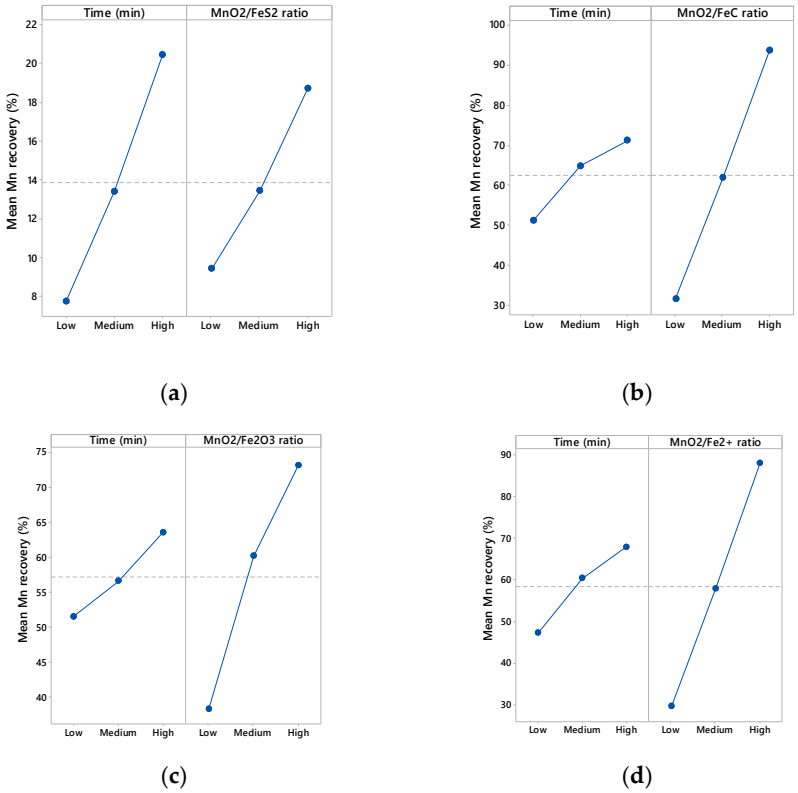

Figure 3. Main effect plots of Mn extraction in function of Time (min) and MnO_2/Reductant agent ratio for (**a**) FeS_2, (**b**) FeC, (**c**) Fe_2O_3 and (**d**) Fe^{2+} agents.

By developing the ANOVA test and the multiple linear regression adjustment for each of the configurations, it is necessary to recover the Mn as a function of the time predictor variables, and MnO_2/reducing agent, which is given by:

$$\text{Mn Extraction (\%) } [FeS_2] = 13.867 + 6.330 \times \text{Time} + 4.648 MnO_2/FeS_2 \times \text{ratio}. \quad (20)$$

$$\text{Mn Extraction (\%) } [Fe^{2+}] = 58.49 + 10.39 \times \text{Time} + 29.22\ MnO_2/Fe^{2+} \times \text{ratio}. \quad (21)$$

$$\text{Mn Extraction (\%) } [FeC] = 62.42 + 10.04 \times \text{Time} + 31.16\ MnO_2/FeC \times \text{ratio}. \quad (22)$$

$$\text{Mn Extraction (\%) } [Fe_2O_3] = 57.22 + 6.01 \times \text{Time} + 17.37\ MnO_2/Fe_2O_3 \times \text{ratio}. \quad (23)$$

The time and ratio MnO_2/reducing agents were coded according to low and medium high levels. From the adjustment of multiple regression models, the interactions of the factors together with the curvature of the time factor and MnO_2/reducing agent did not contribute to explain the variability in any of the adjusted models.

From Equations (20)–(23) and from the main effect graphs in Figure 3, the factor that had showed a higher marginal contribution in Mn recovery was the MnO_2/Reducing agent ratio for the experimental design whose reducing agent was Fe^{2+}, FeC and Fe_2O_3, while in case of using FeS_2 as a reducing agent, the factor that has a greater impact on recovery is time.

The ANOVA test indicates that the models adequately represent Mn extraction for the set of sampled values. The model does not require additional adjustments and is validated by the goodness-of-fit statistics shown in Table 6. The p value ($p < 0.05$) and the significance tests F ($F_{Regression} >> (F_{Table} = F_{2,6}(5.1432))$ for a level of significance of $\alpha = 0.05$ (95% confidence level) indicate that all models generated for the representation of the experimental tests were statistically significant. The normality tests indicate that the assumption of normality of the residuals was met. The low values of the S statistic indicate that there were no large deviations between the experimental data and the values of the adjusted model.

Table 6. Goodness of fit statistics.

Response	F-Value	*p*-Value	S	R^2	R^2 (Pred)
Mn Extraction (%) [FeS_2]	102.13	0.000	1.34602	97.15%	92.65%
Mn Extraction (%) [Fe^{2+}]	145.76	0.000	4.44890	97.98%	95.63%
Mn Extraction (%) [FeC]	116.48	0.000	5.25341	97.49%	94.35%
Mn Extraction (%) [Fe_2O_3]	42.02	0.000	4.91305	93.34%	84.37%

The value of the R^2 statistics was greater than 90%, which indicates that a large part of the total variability was explained by the models, while the similarity between the R^2 and R^2 predictive statistics indicates that the model could adequately predict the response to new observations.

3.2. *Effect on MnO_2/Reducing Agent Ratio*

In Figure 4, results are presented for the dissolution of Mn with the use of different Fe reducing agents at different ratios of Mn/Fe. For all the cases presented (Figure 4a–d), when working at low Mn/Fe ratios the highest recoveries of Mn were obtained. Ratios of 1/2 proved to be an optimum in Figure 4b–d. While for the Figure 4a in ratios of 1/3, the increase in the dissolution of Mn continued. The best results were obtained in Figure 4c when working with FeC because it allowed a high activity ratio through the regeneration of ferrous ions, favoring the dissolution of Mn and allowing better results to the use of Fe^{2+} in a direct way that is presented in Figure 4b. Using Fe_2O_3 shows good results when working with MnO_2/Fe_2O_3 ratios of 1/2, although it is lower than those presented when using Fe^{2+} and FeC. However, this may be an attractive proposal due to the reuse of tailings that are an environmental responsibility. For the use of pyrite, the lowest Mn solutions could be observed in this study. In previous studies [2,22,23,33], it has been indicated that it is not necessary to work at high concentrations of H_2SO_4 in the system to obtain high Mn solutions from marine nodules, but that if it is important to have low Mn/Fe ratios. The results presented in Figure 4a show a progressive increase in the Mn dissolution when increasing the amounts of FeS_2 in the system, however, it may be necessary to increase the acid concentration or temperature because of the kinetics of dissolution of ferrous ions from the pyrite ore.

For the performed tests, the values of potential and pH for the different reducing agents used for Mn/Fe ratios of 1/2 are presented in Figure 5. Senanayake [13] indicated that dissolving Mn from marine nodules requires to work in potential ranges between −0.4 and 1.4 V and pH between −2 and 0.1. With this, it is possible to avoid the precipitation of the Mn through the oxidation-reduction reaction, due to the presence of ferrous and ferric ions [34]. The outcomes met the operational condition mentioned above, which is due to the high concentrations of reducing agent. The lowest potential values were obtained with Fe^{2+} and FeC, wherein the iron (FeC) favored the regeneration of ferrous ions, which allows maintaining low potential ranges [22].

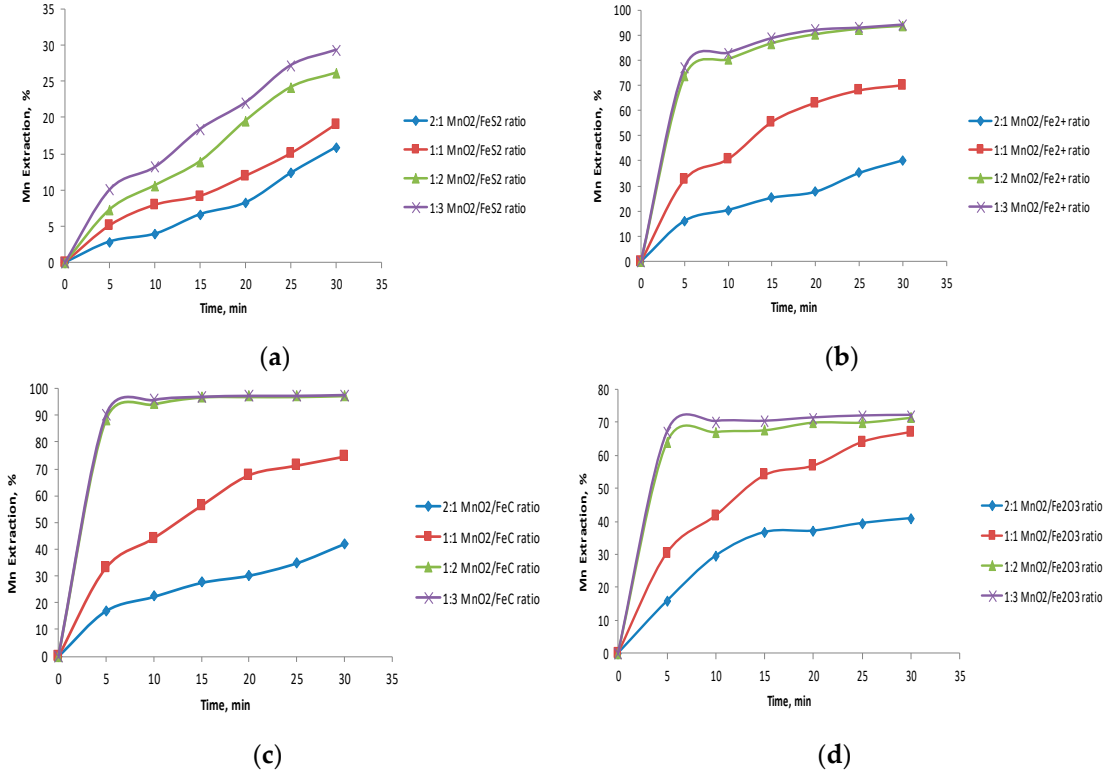

Figure 4. Effect on the ratio of MnO_2/reducing agent at room temperature (25 °C), 0.1 mol/L H_2SO_4, 600 rpm and particle size of −75 + 53 µm (reducing agent: (**a**) FeS_2, (**b**) Fe^{2+}, (**c**) FeC and (**d**) Fe_2O_3).

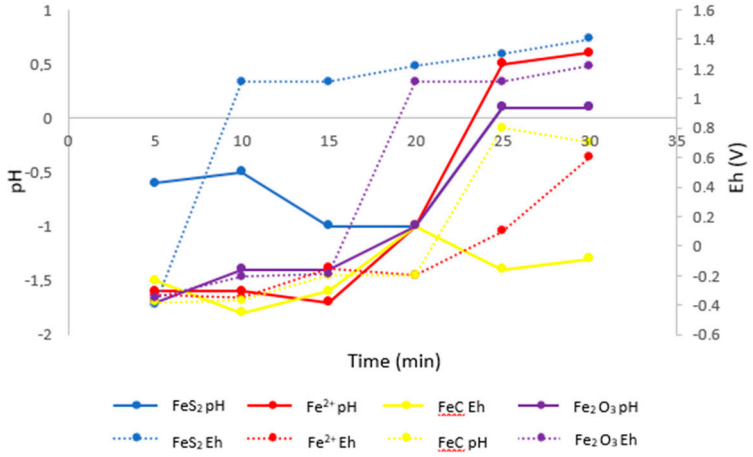

Figure 5. Effect of the potential and pH in the solution of Mn with different reducing agents (MnO_2/Fe_2O_3 ratio of 1/2, 25 °C, 600 rpm, −75 + 53 µm, acid concentration to 0.1 mol/L).

3.3. Effect on the Concentration of H_2SO_4

Figure 6 shows the effect of sulfuric acid concentration when working at Mn/Fe ratios of 1/2 with the use of different Fe reducing agents. Figure 6b,c shows that the concentration of H_2SO_4 was irrelevant in the extraction of Mn when working at low ratios of Mn/Fe with the use of Fe^{2+} and FeC. This is compatible with previous studies conducted by Zakeri et al. [24] and Bafghi et al. [22]. The researchers indicated that working at high concentrations of ferrous ions, variables like acid concentration and particle size were irrelevant. For the case shown in Figure 6d, it was observed that when working with the use of Fe_2O_3 there was a slight increase in Mn solutions when working above 0.1 mol/L, although it was observed that there were no differences between 0.5 and 1 mol/L, which reaffirms what was raised by Saldaña et al. [2], where they indicated that when working on

acid-reducing leaching of MnO_2 using tailings, the acid concentration only influenced the extractions of Mn when it was not operated in high levels of Fe or no temperature increase. Finally, it can be seen in Figure 6a that when working with pyrite, the concentration of acid in the system was important. This was consistent with the results obtained by Kanungo et al. [21], which states that in an acid solution of marine nodules with the use of pyrite as the acidity of the medium decreases, the rate of reduction of MnO_2 decreases.

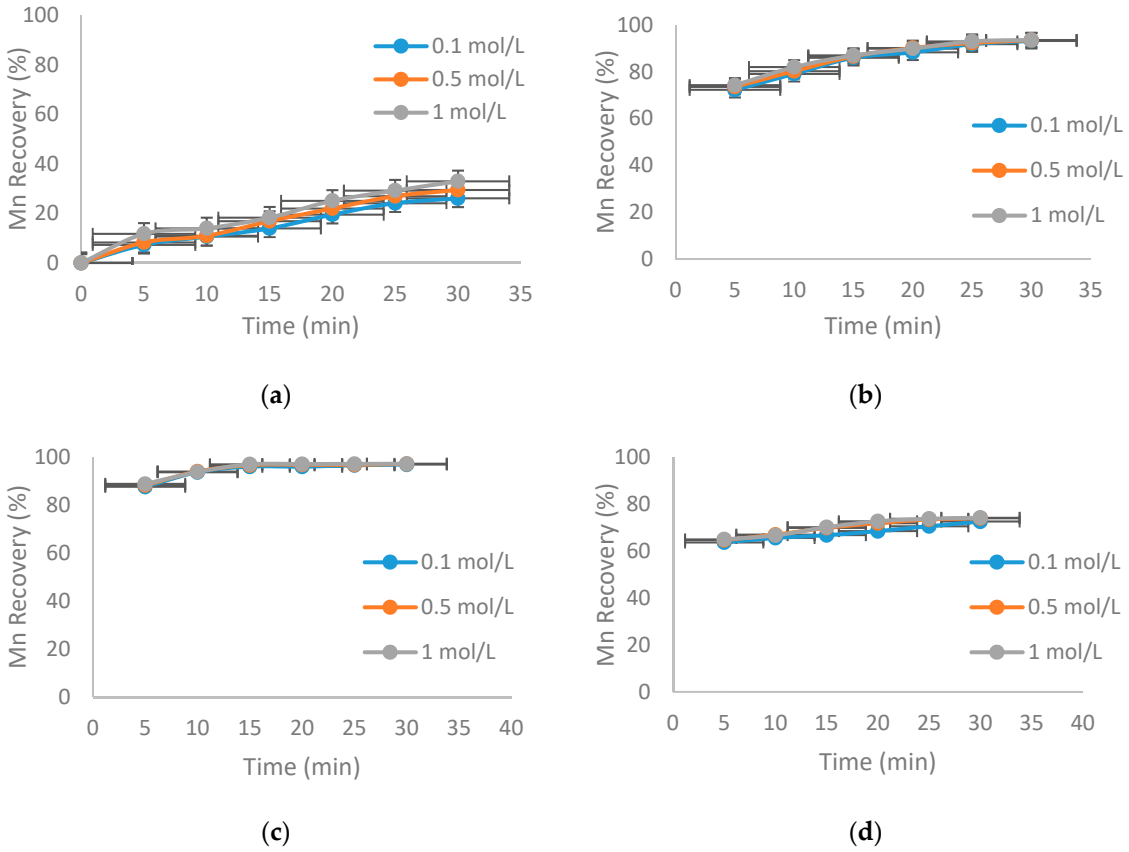

Figure 6. Effect on the concentration of H_2SO_4 at room temperature of (25 °C), ratio of MnO_2/reducing agent of 1/2, 600 rpm and particle size of −75 + 53 µm (reducing agent: (**a**) FeS_2, (**b**) Fe^{2+}, (**c**) FeC and (**d**) Fe_2O_3).

4. Conclusions

The Fe presented in the different additives proved to be a good reducing agent, increasing the dissolution of MnO_2. The main findings of this study were the following:

(1) Fe^0 (FeC) proved to be the best reducing agent for the dissolution of Mn from marine nodules since the direct contact of Fe in the liquid solution kept the regeneration of ferrous ions, due to high levels of ferrous and ferric ions.

(2) When working with Fe^{2+}, FeC and Fe_2O_3, and having high concentrations of reducing agent (MnO_2 ratios/reducing agent 1/2 or lower), low potential values were maintained, which allowed working at low acid concentrations (0.1 mol/L). However, for FeS_2, better results were achieved at higher ratios of MnO_2/FeS_2 (1/3) and acid levels of 1 mol/L, which was possibly due to the refractoriness of pyrite.

(3) For the tests carried out in this study with the different Fe reducing agents, the potential and pH ranges were from −0.4 to 1.4 V and −2 to 0.1, favoring the dissolution of Mn from marine nodules, and avoiding the formation of precipitates of the Fe.

(4) The best results of this research (97% of Mn) were obtained at MnO_2/FeC ratios of 1/2, 0.1 mol/L of H_2SO_4, in a time of 20 min.

In future work, other industrial iron wastes, generated in large industries, should be evaluated to create novel acid-reducing processes of MnO_2. Subsequently, to recover the manganese present in the solution, zero-valent iron (ZVl) is a good alternative. Zero valence iron can be reused, from scraps of the metal finishing industry.

Author Contributions: N.T. and R.I.J. contributed in project administration, M.C., S.N., L.A. and J.C. contributed in investigation and D.T. and N.T wrote paper, M.S. contributed in the data curation and software, P.R. contributed in validation and supervision and review and editing.

Funding: This research received no external funding.

Acknowledgments: The authors are grateful for the contribution of the Scientific Equipment Unit- MAINI of the Universidad Católica del Norte for aiding in generating data by automated electronic microscopy QEMSCAN®and for facilitating the chemical analysis of the solutions. We are also grateful to the Altonorte Mining Company for supporting this research and providing slag for this study, and we thank to Marina Vargas Aleuy of the Universidad Católica del Norte for supporting the experimental tests. Pedro Robles thanks the Pontificia Universidad Católica de Valparaíso for the support provided.

Conflicts of Interest: The authors declare no conflict of interest.

References

1. Marino, E.; González, F.J.; Somoza, L.; Lunar, R.; Ortega, L.; Vázquez, J.T.; Reyes, J.; Bellido, E. Strategic and rare elements in Cretaceous-Cenozoic cobalt-rich ferromanganese crusts from seamounts in the Canary Island Seamount Province (northeastern tropical Atlantic). *Ore Geol. Rev.* **2017**, *87*, 41–61. [CrossRef]
2. Saldaña, M.; Toro, N.; Castillo, J.; Hernández, P.; Trigueros, E.; Navarra, A. Development of an Analytical Model for the Extraction of Manganese from Marine Nodules. *Metals* **2019**, *9*, 903. [CrossRef]
3. Hein, J.R. The Geology of Cobalt-rich Ferromanganese Crusts. In *Deep Sea Minerals: Cobalt-Rich Ferromanganese Crusts, A Physical, Biological, Environmental, and Technical Review*; Secretariat of the Pacific Community (SPC): Noumea, New Caledonia, 2013; pp. 7–14.
4. Hein, J.R.; Mizell, K.; Koschinsky, A.; Conrad, T.A. Deep-ocean mineral deposits as a source of critical metals for high- and green-technology applications: Comparison with land-based resources. *Ore Geol. Rev.* **2013**, *51*, 1–14. [CrossRef]
5. González, F.J.; Somoza, L.; León, R.; Medialdea, T.; de Torres, T.; Ortiz, J.E.; Lunar, R.; Martínez-Frías, J.; Merinero, R. Ferromanganese nodules and micro-hardgrounds associated with the Cadiz Contourite Channel (NE Atlantic): Palaeoenvironmental records of fluid venting and bottom currents. *Chem. Geol.* **2012**, *310*, 56–78. [CrossRef]
6. Josso, P.; Pelleter, E.; Pourret, O.; Fouquet, Y.; Etoubleau, J.; Cheron, S.; Bollinger, C. A new discrimination scheme for oceanic ferromanganese deposits using high fi eld strength and rare earth elements. *Ore Geol. Rev.* **2017**, *87*, 3–15. [CrossRef]
7. Koschinsky, A.; Heinrich, L.; Boehnke, K.; Cohrs, J.C.; Markus, T.; Shani, M.; Singh, P.; Stegen, K.S.; Werner, W. Deep-sea mining: Interdisciplinary research on potential environmental, legal, economic, and societal implications. *Integr. Environ. Assess. Manag.* **2018**, *14*, 672–691. [CrossRef]
8. Ghosh, M.K.; Barik, S.P.; Anand, S. Sulphuric Acid Leaching Of Polymetallic Nodules Using Paper As A Reductant. *Trans. Indian Inst. Met.* **2008**, *61*, 477–481. [CrossRef]
9. Hein, J.R. Manganese nodules. In *Encyclopedia of Marine Geosciences*; Springer: Dordrecht, The Netherlands, 2016; pp. 408–412.
10. Sharma, R. Environmental Issues of Deep-Sea Mining. *Procedia Earth Planet. Sci.* **2015**, *11*, 204–211. [CrossRef]
11. Usui, A.; Nishi, K.; Sato, H.; Nakasato, Y.; Thornton, B.; Kashiwabara, T. Continuous growth of hydrogenetic ferromanganese crusts since 17 Myr ago on Takuyo-Daigo Seamount, NW Paci fi c, at water depths of 800—5500 m. *Ore Geol. Rev.* **2017**, *87*, 71–87. [CrossRef]
12. Jana, R.K.; Pandey, B.D. Ammoniacal leaching of roast reduced deep-sea manganese nodules. *Hydrometallurgy* **1999**, *53*, 45–56. [CrossRef]
13. Senanayake, G. Acid leaching of metals from deep-sea manganese nodules—A critical review of fundamentals and applications. *Miner. Eng.* **2011**, *24*, 1379–1396. [CrossRef]
14. Toro, N.; Pérez, K.; Saldaña, M.; Jeldres, R.I.; Jeldres, M.; Cánovas, M. Dissolution of pure chalcopyrite with manganese nodules and waste water. *J. Mater. Res. Technol.* **2019**, in press. [CrossRef]

15. Randhawa, N.S.; Hait, J.; Jana, R.K. A brief overview on manganese nodules processing signifying the detail in the Indian context highlighting the international scenario. *Hydrometallurgy* **2016**, *165*, 166–181. [CrossRef]
16. Pérez, K.; Toro, N.; Campos, E.; González, J.; Jeldres, R.I.; Nazer, A.; Rodriguez, M.H. Extraction of Mn from Black Copper Using Iron Oxides from Tailings and Fe^{2+} as Reducing Agents in Acid Medium. *Metals* **2019**, *9*, 1112. [CrossRef]
17. Su, H.; Liu, H.; Wang, F.; Lü, X.; Wen, Y. Kinetics of reductive leaching of low-grade pyrolusite with molasses alcohol wastewater in H_2SO_4. *Chin. J. Chem. Eng.* **2010**, *18*, 730–735. [CrossRef]
18. Kanungo, S.B.; Jena, P.K. Reduction leaching of manganese nodules of Indian Ocean origin in dilute hydrochloric acid. *Hydrometallurgy* **1988**, *21*, 41–58. [CrossRef]
19. Khalafalla, S.E.; Pahlman, J.E. Selective Extraction of Metals from Pacific Sea Nodules with Dissolved Sulfur Dioxide. *JOM J. Miner. Met. Mater. Soc.* **1981**, *33*, 37–42. [CrossRef]
20. Han, K.N.; Fuerstenau, D.W. Extraction behavior of metallic elements from deep-sea manganese nodules in reducing medium. *Mar. Min.* **1986**, *2*, 155–169.
21. Kanungo, S.B. Rate process of the reduction leaching of manganese nodules in dilute HCl in presence of pyrite. Part I. Dissolution behaviour of iron and sulphur species during leaching. *Hydrometallurgy* **1999**, *52*, 313–330. [CrossRef]
22. Bafghi, M.S.; Zakeri, A.; Ghasemi, Z.; Adeli, M. Reductive dissolution of manganese ore in sulfuric acid in the presence of iron metal. *Hydrometallurgy* **2008**, *90*, 207–212. [CrossRef]
23. Toro, N.; Herrera, N.; Castillo, J.; Torres, C.; Sepúlveda, R. Initial Investigation into the Leaching of Manganese from Nodules at Room Temperature with the Use of Sulfuric Acid and the Addition of Foundry Slag—Part I. *Minerals* **2018**, *8*, 565. [CrossRef]
24. Zakeri, A.; Bafghi, M.S.; Shahriari, S.; Das, S.C.; Sahoo, P.K.; Rao, P.K. Dissolution kinetics of manganese dioxide ore in sulfuric acid in the presence of ferrous ion. *Hydrometallurgy* **2007**, *8*, 22–27.
25. Kanungo, S.B. Rate process of the reduction leaching of manganese nodules in dilute HCl in presence of pyrite. Part II: Leaching behavior of manganese. *Hydrometallurgy* **1999**, *52*, 331–347. [CrossRef]
26. Toro, N.; Saldaña, M.; Castillo, J.; Higuera, F.; Acosta, R. Leaching of Manganese from Marine Nodules at Room Temperature with the Use of Sulfuric Acid and the Addition of Tailings. *Minerals* **2019**, *9*, 289. [CrossRef]
27. El Problema Global de la Chatarra de Mineral de Hierro se Agrava|Minería en Línea. 2018. Available online: https://mineriaenlinea.com/2018/11/el-problema-global-de-la-chatarra-de-mineral-de-hierro-se-agrava/ (accessed on 26 November 2019).
28. MCH, Reciclaje Minero: En Busca de un Sector Sustentable—Minería Chilena. 2013. Available online: http://www.mch.cl/2013/01/28/reciclaje-minero-en-busca-de-un-sector-sustentable/# (accessed on 25 November 2019).
29. Campos, C. EyN: Reciclaje minero: En busca de un sector sustentable. 2013. Available online: http://www.economiaynegocios.cl/noticias/noticias.asp?id=105240 (accessed on 26 November 2019).
30. Bezerra, M.A.; Santelli, R.E.; Oliveira, E.P.; Villar, L.S.; Escaleira, L.A. Response surface methodology (RSM) as a tool for optimization in analytical chemistry. *Talanta* **2008**, *76*, 965–977. [CrossRef] [PubMed]
31. Montgomery, D.C. *Montgomery: Design and Analysis of Experiments*, 8th ed.; John Wiley & Sons: New York, NY, USA, 2012.
32. Mathews, P.G. *Design of Experiments with MINITAB*; William, A., Ed.; ASQ Quality Press: Milwaukee, WI, USA, 2005; ISBN 0873896378.
33. Toro, N.; Briceño, W.; Pérez, K.; Cánovas, M.; Trigueros, E.; Sepúlveda, R.; Hernández, P. Leaching of Pure Chalcocite in a Chloride Media Using Sea Water and Waste Water. *Metals* **2019**, *9*, 780. [CrossRef]
34. Komnitsas, K.; Bazdanis, G.; Bartzas, G.; Sahinkaya, E.; Zaharaki, D. Removal of heavy metals from leachates using organic/inorganic permeable reactive barriers. *Desalin. Water Treat.* **2013**, *51*, 3052–3059. [CrossRef]